INORGANIC CARBON-LIMITED FRESHWATER ALGAL GROWTH AT HIGH PH: REVISITED WITH FOCUS ON ALKALINITY

Mary Katherine Watson[1,*], Elizabeth Flanagan[2], Caye Drapcho[2]

[1] Civil and Environmental Engineering, The Citadel, Charleston, South Carolina, USA.
[2] Biosystems Engineering Program, Department of Environmental Engineering and Earth Sciences, Clemson University, Clemson, South Carolina, USA.
[*] Correspondence: mwatson9@citadel.edu

HIGHLIGHTS

- Non-carbonate components of BG11 media impact TIC calculation on average 4.00 mg/L at high pH.
- BG11 media non-carbonate alkalinity (NCA) varies with pH: NCA (meq/L) = $0.0393\times e^{0.2075\times pH} + (2.086\times 10^{-9})e^{1.860\times pH}$.
- Monod kinetic constants with CO_2, HCO_3^-, and CO_3^{2-} as inorganic carbon sources are improved from a previous report.
- Kinetic constants continue to be the only known reports considering multiple inorganic carbon sources.
- Algal stoichiometric reactions are developed that account for variation in cell content and carbon source.

ABSTRACT. *Due to increasing atmospheric CO_2, algal growth systems at high pH are of interest to support enhanced diffusion and carbon capture. Given the interactions between algal growth, pH, and alkalinity, data from Watson and Drapcho (2016) were re-examined to determine the impact of the non-carbonate constituents in BG11 media on estimates of Monod kinetic parameters, biomass yield, and cell stoichiometry. Based on a computational method, non-carbonate alkalinity (NCA) in BG11 media varies with pH according to: NCA (meq/L) = $0.0393\times e^{0.2075\times pH} + (2.086\times 10^{-9})e^{1.860\times pH}$ ($R^2 = 0.999$) over the pH range of 10.3 – 11.5. Updated maximum specific growth rates were determined to be 0.060, 0.057, and 0.051 hr^{-1} for CO_2, HCO_3, and CO_3, respectively. Generalizable stoichiometric algal growth equations that consider variable nutrient ratios and multiple inorganic carbon species were developed. Improved kinetic and stoichiometric parameters will serve as the foundation for a dynamic mathematical model to support the design of high pH algal carbon capture systems.*

Keywords. *Algae, Alkalinity, Carbon Abatement, Carbon Capture, Kinetics, Stoichiometry, Total Inorganic Carbon.*

The current atmospheric carbon dioxide (CO_2) concentration is higher than at any other time in the past 800,000 years, with levels continuing to rise due to the combustion of fossil-based fuels and changing land use (Lindsey, 2021). As a greenhouse gas, CO_2 accumulation in the atmosphere is leading to global climate change, with temperatures rising by 0.08°C each decade since 1880 (Lindsey, 2021). The total 2°C increase in average surface temperature is already leading to many interconnected ecological, social, and economic impacts, such as flooding/drought, disease spread, ocean acidification, and infrastructure damage (NOAA, 2021).

The Office of Fossil Energy and Carbon Management has identified Carbon Dioxide Removal and Conversion (CDRC), including biomass with carbon removal and storage, as a group of technologies to support a future net-zero carbon economy (Office of Fossil Energy & Carbon Management , 2022). Microalgae are especially suited for carbon capture because their photosynthetic capacity is typically 10%-20%, which is substantially greater than that of terrestrial plants (1%-2%) (Singho and Ahluwalia, 2013).

Algal growth at high pH is an under-explored approach for improving carbon capture. The authors of an early Department of Energy (DOE) report first contemplated "the feasibility of large, alkaline freshwater systems to exploit pH and increase CO_2 diffusion rates" (Reichle et al., 1999). Based on film theory, a gas can be absorbed into a liquid via unenhanced or kinetically-enhanced diffusion (e.g., Danckwerts, 1970; Smith, 1985). During unenhanced diffusion, CO_2 remains inert as it moves through the boundary layer. However, at high pH, CO_2 remains in the boundary layer long enough for hydroxylation reactions to occur (Portielje and Lijklema, 1995). Chemical consumption of CO_2 at the air-water interface increases CO_2 diffusion and availability for biofixation (Reichle et al., 1999). High pH conditions can be naturally encouraged through the provision of nitrate as a nitrogen source, the consumption of which is known to increase culture pH and alkalinity (Touloupakis et al., 2016).

Submitted for review on 17 October 2022 as manuscript number NRES 15411; approved for publication as a Research Article by Associate Editor Dr. Debabrata Sahoo and Community Editor Dr. Kati Migliaccio of the Natural Resources & Environmental Systems Community of ASABE on 3 July 2023.

  ISSN 2769-3295 https://doi.org/10.13031/ja.15411

A tool is needed to forecast the complex interactions between chemical, physical, and biological factors impacting the design and operation of high pH algal carbon capture systems. As pH increases, CO_2 diffusion increases and CO_2 concentration decreases. The kinetic roles of HCO_3^- and CO_3^{2-} as inorganic carbon sources are poorly understood, despite a decades-long debate in the literature (e.g., King, 1970; Novak and Brune, 1985; Chen and Durbin, 1994). Further, algal growth is known to impact culture pH and alkalinity, affecting growth rates and the diffusion of atmospheric CO_2.

Watson and Drapcho (2016) presented stoichiometric and kinetic parameters for a green algal culture, determined using calculated values of total inorganic carbon concentration (TIC) based on alkalinity titrations in BG-11 media, to serve as the basis for such a dynamic model. However, subsequent analysis showed that media ionic strength and non-carbonate buffers cannot be neglected when calculating TIC in BG11 media, suggesting the need for re-assessment of kinetic parameters, yield values, and biomass stoichiometry.

Thus, this paper aims to extend the work of Watson and Drapcho (2016) to build toward a dynamic algal growth model specifically adapted for high-pH systems. The objectives are to: (1) develop a method for calculating TIC from total alkalinity measured in BG11 media; (2) build generalizable stoichiometric algal growth equations that consider variable nutrient ratios and multiple inorganic carbon species; and (3) re-examine Watson and Drapcho (2016) data based on an improved understanding of BG11 media composition and algal growth stoichiometry.

Literature Review and Analysis

Alkalinity, TIC speciation, and algal growth are interconnected. Algal growth is known to alter system alkalinity due to the uptake of nitrogen and phosphorous, but algal cell stoichiometric representations are often based on non-representative C:N:P ratios. A critical literature review and analysis was conducted to develop relationships describing alkalinity, TIC speciation, and algal growth, especially for high pH systems that may be well-suited for carbon abatement.

Alkalinity and Inorganic Carbon in Complex Systems

Relationship between Alkalinity and Inorganic Carbon

While the concept of alkalinity as the acid-neutralizing capacity of water is straightforward, its application requires more consideration. Dickson defined total titrimetric alkalinity as "a measure of the proton deficit of the solution relative to an arbitrarily defined zero level of protons" (1981). While several proton reference levels are reported in the literature, Dickson (1981) defends a titration endpoint of pH 4.5, such that acids and bases with dissociation constants above and below pK_a of 4.5 are considered proton donors and acceptors, respectively. Defined as such, alkalinity is a capacity factor (measured in units of concentration rather than activity) that is conservative against physical changes, but consumed and created through various biogeochemical processes (Stumm and Morgan, 1996; Wolf-Gladrow et al., 2007).

Measured pH and total alkalinity values have been used extensively to calculate TIC (eqs. 1-5) in freshwater ecosystems (Stumm and Morgan, 1996), aquaculture systems (Boyd et al., 2016; Drapcho and Brune, 2000), and algal systems designed for carbon capture (Watson and Drapcho, 2016; Ataeian et al., 2019; Vadlamani et al 2017). Total alkalinity is measured through titration to pH 4.5, per Standard Method 2320 (APHA, 1995), such that the added acid is proportional to the bases consumed. Alkalinity is then expressed as a function of HCO_3^- and CO_3^{2-} concentration (eq. 2). Subsequently, TIC and individual carbon species are calculated per equations 2-5 (Stumm and Morgan, 1996).

$$ALK = \left[HCO_3^-\right] + 2\left[CO_3^{2-}\right] + \left[OH^-\right] - \left[H^+\right] \quad (1)$$

$$TIC = \frac{ALK - \left[OH^-\right] + \left[H^+\right]}{\alpha_{1,TIC} + 2\alpha_{2,TIC}} \quad (2)$$

$$\alpha_{0,TIC} = \left[H_2CO_3^*\right] / \left[TIC\right] \quad (3)$$

$$\alpha_{1,TIC} = \left[HCO_3^-\right] / \left[TIC\right] \quad (4)$$

$$\alpha_{2,TIC} = \left[CO_3^{2-}\right] / \left[TIC\right] \quad (5)$$

Inherent in equation 1 is the assumption that TIC species (i.e., carbonate alkalinity) and hydroxyl ions are the only significant contributors to total alkalinity. However, in laboratory media, polluted waters, or seawater, non-carbonate buffers can contribute to measured total alkalinity and inflate calculated values of TIC.

Informed by Dickson (1992), the analysis below outlines a computational approach to consider the impact of non-carbonate buffers in BG11 media on TIC calculation. Dissociation constants for BG11 non-carbonate buffers were examined, taking into account proton reference levels, as discussed in Dickson (1981, 1992) and Wolf-Gladrow et al. (2007). These constants were then employed to construct a total alkalinity equation that accounts for non-carbonate acids and bases. Subsequently, non-carbonate alkalinity can be subtracted from total alkalinity prior to TIC calculation.

Impact of Non-Carbonate Buffers in BG11 Media

BG11 media is commonly used in laboratory systems for algae cultivation. It contains an excess of macronutrients and micronutrients, many of which act as acids and bases (table 1). Of the 13 non-carbonate BG11 components, 5 are present in quantities that impact total alkalinity titrations (table 2). Proton reference levels are determined by comparing pK_a values for each acid/base system with the endpoint of pH 4.5. For borate with pK_a values of 9.2, 12.4, and 13.4, nearly all is present as H_3BO_4 at pH 4.5 (even after accounting for ionic strength). Proton reference levels for ammonia, molybdate, and phosphate are determined similarly. For citrate, with pK_a values of 3.1, 4.8, and 6.4, both H_2-citrate$^-$ and H-citrate^{2-} would be present at pH 4.5.

For each buffering system, species are compared to the reference compound and assigned a coefficient that describes how many protons would be accepted upon titration

Table 1. Chemical characteristics of BG11 media components (sodium carbonate excluded).

BG11 Media Component	Acid/ Base System	Dissociation Constant(s) (pK_a values) (Stumm and Morgan, 1996)	Reference Compound(s) at pH 4.5
K_2HPO_4	H_3PO_4/ PO_4^{3-}	2.1, 7.2, 12.4	$H_2PO_4^-$
H_3-citrate ($C_6H_8O_7$)	H_3-citrate/citrate^{3-}	3.1, 4.8, 6.4	H_2-citrate$^-$, H-citrate^{2-}
$(NH_4)_5[Fe(C_6H_4O_7)_2]$	NH_4^+ /NH_3	9.25[a]	NH_3
H_3BO_3	H_3BO_3/ BO_3^{3-}	9.2, 12.4, 13.3	H_3BO_3
Na_2MoO_4*$2H_2O$	H_2MoO_4/MoO_4^{2-}	3.6 – 4.0, 3.9 – 4.4	H_2MoO_4[b]
$EDTA^{4-}$	H_4EDTA/EDTA4-	0, 1.5, 2.0, 2.7	No measurable contribution to alkalinity
$NaNO_3$	HNO_3/NO_3^-	< 1	
$Co(NO_3)_2$*$6H_2O$			
$MgSO_4$*$7H_2O$	H_2SO_4/SO_4^{2-}	-2.8, 2	
$ZnSO_4$*$7H_2O$			
$CuSO_4$*$5H_2O$			
$CaCl_2$*$2H_2O$	Not applicable		
$MnCl_2$*$4H_2O$			

[a] pK_a = ammonium.
[b] Assumption made for simplicity, since very little sodium molybdate present. In reality, H_2MoO_4 and $HMoO_4^-$ present at pH 4.5.

Table 2. Alkalinity contribution equations of various media components.[a]

Buffering System	Alkalinity Contribution at Endpoint pH 4.5
Phosphate	$\alpha_{1,PO4}\left\{\left[HPO_4^{2-}\right]+2\left[PO_4^{3-}\right]-\left[H_3PO_4\right]\right\}+\alpha_{2,PO4}\left\{\left[PO_4^{3-}\right]-\left[H_2PO_4^-\right]-2\left[H_3PO_4\right]\right\}$
Citrate	$\alpha_{1,citrate}\left\{\left[H\cdot citrate\right]+2\left[citrate^{3-}\right]-\left[H_3\cdot citrate\right]\right\}+\alpha_{2,citrate}\left\{\left[citrate^{3-}\right]-\left[H_2\cdot citrate\right]-2\left[H_3\cdot citrate\right]\right\}$
Ammonium	$\left[NH_4^+\right]$
Borate	$\left[H_2BO_3^-\right]+2\left[HBO_3^{2-}\right]+3\left[BO_3^{3-}\right]$
Molybdate	$\left[HMoO_4^-\right]+2\left[MoO_4^{2-}\right]$

[a] $\alpha_{1,PO4}$ = [$H_2PO_4^-$]/[total PO_4^{3-}]; $\alpha_{2,PO4}$ = [HPO_4^{2-}]/[total PO_4^{3-}]; $\alpha_{1,citrate}$ = [H_2-citrate]/[total citrate]; α_2-citrate = [H-citrate/total citrate]

to pH 4.5 (table 2). For the borate-system, H_3BO_4 would lose a proton upon titration to $H_2BO_3^-$, while HBO_3^{2-} and BO_3^{3-} would accept one and two protons, respectively. Non-carbonate contributions of ammonia, phosphate, and molybdate are formulated similarly. For citrate, non-carbonate alkalinity expressions are generated for both proton reference levels and weighted based on the relative amounts of H_2-citrate$^-$ ($\alpha_{1,citrate}$) and H-citrate^{2-} ($\alpha_{2,citrate}$) present at pH 4.5.

The total alkalinity of BG11 media can be expressed as the sum of carbonate alkalinity, non-carbonate alkalinity, and water alkalinity (eq. 6). In high pH systems, metal solids and hydroxides will likely be formed, although their contributions to total alkalinity are expected to be small (ALK_{solids} and $ALK_{OH,compounds}$). Ultimately, equation 6 can be used to convert total (titrimetric) alkalinity to carbonate alkalinity, which allows for the accurate calculation of TIC from equation 2.

$$\begin{aligned} ALK_{total} = & \\ &\left[ALK_{carbonate}\right]+\left[ALK_{phosphate}\right]+\left[ALK_{citrate}\right] \\ &+\left[ALK_{ammonia}\right]+\left[ALK_{borate}\right]+\left[ALK_{molybdate}\right] \\ &+\left[ALK_{OH,compunds}\right]+\left[ALK_{solids}\right]+\left[OH^-\right]-\left[H^+\right] \end{aligned} \quad (6)$$

Algal Growth Stoichiometry – Interaction with Alkalinity

Classic Algal Growth Stoichiometry

In the early 20th century, Redfield (1934) found that molar C:N:P ratios were 106:16:1 ("Redfield ratios") throughout the oceans. The discovery of Redfield ratios is regarded as one of the most "profound" discoveries in oceanography (Planavsky, 2014). Later, Redfield ratios were operationalized by creating a balanced stoichiometric equation to describe algal growth (eq. 7). Anderson (1995) cites that Richards (1965) may have been the first to publish equation 7, which was popularized by Stumm and Morgan (1996). Equation 7 depicts the uptake of macronutrients (CO_2, NO_3^-, HPO_4^{2-}) during the production of algal biomass with Redfield Ratios ($C_{106}H_{263}O_{110}N_{16}P$). Further, equation 7 illustrates the impact of algal growth on system alkalinity, including an increase in alkalinity (uptake of protons) when nitrate is used as the nitrogen source. Overall, Stumm and Morgan (1996) commentate that the simple relationship between nitrogen, phosphorous, and oxygen evolution in aquatic ecosystems is evidence of "Liebig's Law of the Minimum."

$$\begin{aligned} &106CO_2+16NO_3^-+HPO_4^{2-}+18H^++122H_2O \\ &\xleftarrow[respiration]{photosynthesis}C_{106}H_{263}O_{110}N_{16}P+138O_2 \end{aligned} \quad (7)$$

Importance of C:N:P Ratios and Alkalinity Implications

While Redfield ratios remain commonly used and powerful, especially for deep marine systems (Auguères and Loreau, 2015), deviations have been widely documented. Laboratory marine cultures showed C:N ratios to be close to 106:6 only under nutrient-replete conditions, although N:P ratios were often quite different from 16:1, perhaps due to the accumulation of inorganic polyphosphates (Geider and La Roche, 2002). Furthermore, variations were even more significant under nutrient-deplete conditions, with N:P typically less than 5 and over 100 under nitrogen-limiting

and phosphorus-limiting conditions, respectively (Geider and La Roche, 2002). Similarly, Hillebrand et al. (2013) showed N:P in marine phytoplankton to decrease with increasing specific growth rate, based on an analysis of 55 data sets.

Deviations from Redfield ratios are also prevalent among freshwater algae. Redfield himself found the phosphorus content of seven species of green algae cultured under identical nutrient conditions to vary significantly (Ketchum and Redfield, 1949). Interestingly, C:N ratios were similar across species and somewhat close to the Redfield ratio for freshwater phytoplankton (table 3).

Given that cellular macronutrients vary based on culture conditions and algal species, general stoichiometric equations are needed to model the molecular formula for biomass. Generic C:N:P molar values, expressed as x:y:1, can be calculated based on the measured mass of C, N, and P per mass of biomass (designated as X, Y, and Z, respectively), as shown in equations 8 and 9.

$$\text{"x"}\frac{\text{mol C}}{\text{mol biomass}} = \left(\text{"X"}\frac{\text{g C}}{\text{g biomass}}\right)_{\text{measured}}\left(\frac{\text{mol C}}{12.01\text{g C}}\right) \div\left(\text{"Z"}\frac{\text{g P}}{\text{g biomass}}\right)_{\text{measured}}\left(\frac{\text{mol P}}{30.97\text{ g P}}\right) \quad (8)$$

$$\text{"y"}\frac{\text{mol N}}{\text{mol biomass}} = \left(\text{"Y"}\frac{\text{g N}}{\text{g biomass}}\right)_{\text{measured}}\left(\frac{\text{mol N}}{14.01\text{g N}}\right) \div\left(\text{"Z"}\frac{\text{g P}}{\text{g biomass}}\right)_{\text{measured}}\left(\frac{\text{mol P}}{30.97\text{ g P}}\right) \quad (9)$$

Equation 7 can be rebalanced based on a generic C:N:P ratio (eq. 10), with carbon dioxide reflected as the inorganic carbon source. Nitrate is used as the sole nitrogen source, although the exercise could be repeated for ammonium. For the phosphorus source, HPO_4^{2-} is shown, although other authors show different forms of phosphate are used by algae (e.g., Brewer and Goldman, 1976; Paulmier et al., 2009). Subsequent analysis shows that the choice of phosphate source is mathematically unimportant to alkalinity.

Table 3. Elemental composition of several freshwater green algae cultured under uniform nutrient conditions in a laboratory (adapted from Ketchum and Redfield, 1949).[a]

	Mass Composition (Dry Weight Basis,%)			Molar Ratios		
Species	Carbon	Nitrogen	Phosphorous	C:P	N:P	C:N
S. obliquus no. 1	44.9	6.9	3.9	29.6	3.9	7.5
S. obliquus no. 2	47.8	7.9	2.5	48.7	6.9	7.0
S. basilensis	47.0	7.7	8.6	14.2	2.0	9.2
C. pyrenoidosa	48.3	7.1	2.7	46.3	5.8	7.9
C. vulgaris	46.8	7.1	2.6	46.7	6.1	7.6
Redfield Ratios	-	-	-	106	16	6.6

[a] Carbon and nitrogen content on a dry-weight basis calculated from reported values on an ash-free basis and ash content.

$$xCO_2 + yNO_3^- + zHPO_4^{2-} + (y+2z)H^+ + (x+y)H_2O \xleftrightarrow[respiration]{photosynthesis} (CH_2O)_x(NH_3)_y \times (H_3PO_4)_z(micronutrients) + \frac{1}{2}(2x+4y)O_2 \quad (10)$$

The general algal growth equation is congruent with the "nutrient-H^+-compensation principle" proposed by Wolf-Gladrow et al. (2007) and indirectly described by Wang and Curtis (2016). Since algae often obtain nutrients in the form of anions, they must expel cations to maintain electroneutrality. While Wolf-Gladrow et al. (2007) consider a variety of ion exchanges, they conclude proton pumps (or hydroxyl pumps in the opposite direction) are responsible for ensuring electroneutrality. As such, proton uptake is shown during photosynthesis (eq. 10), although the production of hydroxyl ions would be mathematically equivalent.

Nitrate uptake results in equal alkalinity production on a mol-equivalent basis. Equation 10 shows that uptake of "y" mol of nitrate results in uptake of "y" mol of protons (i.e., "+ y" mol-equivalents of alkalinity). Wolf-Gladrow et al. (2007) note that Brewer and Goldman (1976) and Goldman and Brewer (1980) verify that one mol of nitrate uptake produces one mol-equivalent of alkalinity in laboratory cultures.

While the impact of phosphorous uptake on alkalinity is less-studied, the nutrient-H^+-compensation principle supports that any form of phosphorous uptake results in equal alkalinity production on a mol-equivalent basis (Wolf-Gladrow et al., 2007). At an alkalinity endpoint of pH 4.5 (where nearly all phosphorous exists at $H_2PO_4^-$), direct uptake of "z" mol of HPO_4^- represents a "z" mol-equivalent reduction in alkalinity ("-z" mol-equivalents). Also, uptake of "z" mol of HPO_4^{2-} results in a "2z" uptake of protons (i.e.,"+2z" mol-equivalents). Combined, "z" mol of HPO_4^{2-} uptake itself results in "z" mol of alkalinity production ("+z" mol-equivalents).

Generalization for Multiple Inorganic Carbon Sources

A long-standing debate exists in the literature concerning the TIC specie(s) used by algae for growth. At a cellular level, CO_2 is the substrate used directly by RuBisco, the enzyme that catalyzes the first reaction in CO_2 fixation (Cooper et al., 1969). Early Monod-based kinetic studies often revealed conflicting results concerning the impact of TIC species on algal growth. The earliest works supported CO_2 only as limiting (e.g., Osterhout and Haas, 1918). Other authors later agreed, including King (1970), Novak and Brune (1985), and Chen and Durbin (1994). In contrast, Goldman et al. (1974) supported a Monod relationship between growth rate and TIC. A limited number of early researchers proposed that CO_3^{2-} may be a substrate for algal growth, but did not provide definitive evidence (Osterlind, 1948; Burlew, 1953; Felfoldy, 1960). The discovery of carbon concentrating mechanisms (CCMs) has provided a molecular basis for HCO_3^- uptake, although little work has been done to explore whether or not CO_3^{2-} can cross the cell membrane (Colman et al., 2002; Bhatti and Colman, 2008).

As CO_2 may not be the sole inorganic carbon source for many types of algae, stoichiometric equations were developed to capture the impacts of HCO_3^- (eq. 11) and CO_3^{2-} (eq. 12) on growth. Equations 11 and 12 illustrate that alkalinity is not impacted by the TIC source. For example, the uptake of "x" mol of bicarbonate represents the removal of "x" mol-equivalents of alkalinity but is accompanied by uptake of "x" mol of protons. Consequently, only algal uptake of nitrate and phosphate impacts alkalinity. These equations can be used in models describing the uptake of TIC sources other than CO_2.

$$xHCO_3^- + yNO_3^- + zHPO_4^{2-} + (x+y+2z)H^+ + (y)H_2O \xleftarrow[respiration]{photosynthesis} (CH_2O)_x(NH_3)_y \times (H_3PO_4)_z(micronutrients) + \frac{1}{2}(2x+4y)O_2 \quad (11)$$

$$xCO_3^{2-} + yNO_3^- + zHPO_4^{2-} + (2x+y+2z)H^+ + (2x+y-2z)H_2O \xleftarrow[respiration]{photosynthesis} (CH_2O)_x \times (NH_3)_y(H_3PO_4)_z(micronutrients) + \frac{1}{2}(2x+4y)O_2 \quad (12)$$

Role of Cellular Micronutrients and Other Macronutrients

The formulation of algal biomass in equations 10-12 neglects micronutrient content, which may lead to an underestimate of molar mass. Although the exact composition of algae is difficult to measure because biomass is often bound with other solids, Stumm and Morgan (1996) propose that the elemental composition should include trace elements (i.e., $C_{106}H_{263}O_{110}N_{16}P_1Si_xFe_aMn_bZn_cCu_dCd_eNi_f$). Grobbelaar (2004) comments that the elemental content of algae is reflective of their environment, with nutrients serving as macronutrients or micronutrients depending on the species and growth conditions. Since total non-silica micronutrient content ranges from 0.36% to 33% (table 4), accounting only for cellular CNPOH could leave much of the cellular mass unaccounted for.

Table 4. Range of the elemental composition of autotrophic algae (from Grobbelaar, 2004; Prochazkova et al., 2014).

	Dry Weight Composition (%)		
Nutrient	Low	Average	High
C	17.5	41.3	65.0
O	20.5	26.8	33.0
H	2.90	6.95	11.0
N	1.00	7.50	14.0
P	0.05	1.68	3.30
Na	0.04	2.37	4.70
K	0.10	3.80	7.50
Ca	0	4.00	8.00
S	0.15	0.88	1.60
Mg	0.05	3.78	7.50
Fe	0.02	1.71	3.40
Zn	0.0005	0.0503	0.1000
Mn	0.002	0.013	0.024
Si	0	11.5	23.0
Mo	0.00002	0.01250	0.02500
Cu	0.0006	0.0153	0.0300
Co	0.00001	0.01000	0.02000
Se	0	0.045	0.090

Implications for Practical Use of Stoichiometric Equations

As long as carbon, nitrogen, and phosphorous are the major macronutrients (and measurements of cellular content are available), equations 10-12 can be used to accurately capture the impacts of algal growth on alkalinity without relying on Redfield ratios. Based on the nutrient-H^+-compensation principle, alkalinity impacts are dependent only on the stoichiometric coefficients for H^+, HCO_3^-, CO_3^{2-}, NO_3^-, and HPO_4^{2-} uptake. Per Anderson (1995), the model of $(CH_2O)_x(NH_3)_y(H_3PO_4)$ could lead to errors in cellular hydrogen and oxygen content. While such errors would impact stoichiometric estimates of oxygen evolution, alkalinity predictions would not be impacted.

However, neither the exact cellular hydrogen, oxygen, nor other non-CNP content needs to be known to estimate the molecular mass of algal biomass. Cellular carbon, nitrogen, or phosphorous measurement will yield the mass of each element per mass of biomass (on either a dry-weight or ash-free-dry-weight basis). The known amount of carbon, for example, per mass of biomass ("X") can be used to calculate the true molecular mass, which allows for the accurate conversion of molar biomass production from equations 10-12 to a mass-basis (eq. 13).

$$\text{Algal Molecular Mass} = \left(12.01\frac{\text{g C}}{\text{mol C}}\right)\left("x"\frac{\text{mol C}}{\text{mol biomass}}\right) \div \left("X"\frac{\text{g C}}{\text{g biomass}}\right)_{measured} \quad (13)$$

METHODS

Data from Watson and Drapcho (2016) were used to investigate both the improved relationship between non-carbonate alkalinity and TIC calculation and the revised algal biomass stoichiometry. This process is described below.

WATSON AND DRAPCHO (2016) CULTURE AND ANALYSIS METHODS

Watson and Drapcho (2016) report on the culture of eight 4L batch algal reactors containing primarily *Scenedesmus*. Cultures were provided with BG11 media modified to include eight levels of initial Na_2CO_3: 0.025, 0.050, 0.075, 0.100, 0.125, 0.150, 0.175, and 0.200 g/L. Media prior to Na_2CO_3 addition was prepared one day in advance. Na_2CO_3 was added to each reactor, pH was measured, and strong acid or base was added to adjust pH to 10.30. Subsequently, reactors were immediately closed with a stopper containing Ascarite II, such that headspace pressure could equilibrate with the atmosphere without allowing CO_2 entry. All reactors were maintained in a controlled-environment room at 25°C with 26.4 W/m^2 (121 µmol/m^2-s) continuous average photosynthetically active radiation at the original liquid level. Reactors were mixed continuously with magnetic stir bars at 300 rpm. Reactor samples were analyzed to characterize TIC and biomass concentrations (table 5).

Table 5. Experimental methods from Watson and Drapcho (2016), with summary of data analysis improvements.

Parameter	Equipment & Method	Sampling Frequency	Needed Adjustments
pH	pH electrode and meter with 3-point calibration	Daily	$[H^+]$ corrected for ionic strength.
Total Alkalinity	Titration with 0.02 or 0.1 N H_2SO4 per Standard Method 2320B (APHA, 1995)	Daily	Subtract non-carbonate alkalinity from total alkalinity before TIC calculation.
Optical Density (OD)	Measured at 750 nm with spectrophotometer and converted to TSS[a]	Daily	None.
Biomass C & N (on mass-basis)	Combustion analyzer	End of Experiments	Express %C,%N,%P as a function of adjusted initial TIC. Calculate biomass yield using adjusted molecular mass.
Biomass P (on mass-basis)	Inductively coupled mass spectrometry		

[a] Using standard curve of OD versus total suspended solids (TSS), per Standard Method 2540D (APHA, 1995).

Adjusting TIC Calculation Based on Non-carbonate Alkalinity and Ionic Strength

The TIC concentrations reported by Watson and Drapcho (2016) were investigated based on the presence of non-carbonate buffers and ionic strength using Visual Minteq software (Gustafsson, 2011). Data adjustments were conducted in four phases: (1) construction and verification of the BG11 media matrix in Minteq, (2) use of Minteq to quantify the impacts of precipitates and hydroxide compounds on total alkalinity, (3) calculation of non-carbonate alkalinity and adjusted TIC at time zero for each reactor, and (4) calculation of non-carbonate alkalinity and adjusted TIC at all subsequent experimental pH values. The detailed process for determining BG11 non-carbonate alkalinity (table 6) is provided in the Supplemental Information.

Non-Carbonate Alkalinity and False TIC as a Function of pH

Using SigmaPlot 15.0 (Systat Software, Inc.; San Jose, CA), nonlinear regression equations were generated to facilitate the estimation of non-carbonate alkalinity as a function of pH. The ionic strength of the BG11 media (with added carbonate) varies only slightly from 0.20 to 0.23 over the experimental pH range of 10.30 to 11.51 (see Supplemental Information). Non-carbonate alkalinity varies exponentially between pH 10.30 and 11.51 (fig. 1). Once non-carbonate alkalinity is determined, TIC and speciation can be estimated based on pH (figs. 2a-c). Thus, TIC in BG11 media at high pH can be estimated from total alkalinity without the use of Minteq.

Table 6. Non-carbonate alkalinity and false[a] TIC in the 0.2 g/L Na_2CO_3 reactor at pH 10.30 and 11.51.

	pH = 10.30		pH = 11.51	
BG11 Media Component	Alkalinity Contribution (mmol/L)	Excess TIC (mg/L C)	Alkalinity Contribution (mmol/L)	False TIC (mg/L C)
Phosphate[b]	0.344	2.48	0.358	2.19
Citrate	0.0794	0.573	0.0794	0.485
Ammonia	0.0558	0.402	0.0611	0.373
Borate	0.0431	0.311	0.0461	0.281
Iron-based solids	0.00932	0.0672	0.00987	0.0603
Mg-hydroxides	0.00529	0.0382	0.00173	0.0106
Molybdate	0.00322	0.0233	0.00322	0.0197
Brucite	0	0	0.323	1.97
Mn-hydroxides	-	-	0.00537	0.0328
Zn-hydroxides	-	0.000576	0.00189	0.0115
TOTAL	0.540	3.90	0.890	5.43

[a] Excess TIC refers to the amount of inorganic carbon that would be incorrectly calculated if non-carbonate alkalinity were not subtracted from total (titrimeric) alkalinity.

[b] From aqueous species and precipitate.

Determination of Kinetic and Stoichiometric Parameters

Monod kinetic and stoichiometric parameters reported in Watson and Drapcho (2016) were re-evaluated using adjusted TIC data. While specific growth rates (μ) for each reactor remained unchanged, non-linear regression was repeated to determine the maximum specific growth rate (μ_{max}) and half-saturation constants for each TIC species ($K_{S,CO2}$, $K_{S,HCO3}$, and $K_{S,CO3}$), per methods provided in Watson and Drapcho (2016). The observed biomass yield (Y_{obs}) for each reactor was determined as the linear regression slope relating biomass to TIC. Finally, linear and/or non-linear regressions were used to generate empirical relationships between biomass elemental composition on a percent-basis to adjusted initial TIC. IBM SPSS Statistics 27 (Chicago, IL) was used for all statistical analyses.

Based on an expanded understanding of the stoichiometry of TIC-limited algal growth (presented above), theoretical biomass yields ($Y_{theoretical}$) were also re-evaluated. First, carbon, nitrogen, and phosphorous biomass content were converted from a mass-basis to a molar-basis using equations 8-9. Next, $Y_{theoretical}$ was calculated on a molar basis for each reactor (mol C/mol biomass). Finally, the molecular mass of algae in each reactor was quantified using equation 13 to allow for the conversion of $Y_{theoretical}$ to a mass-basis (mg C/mg biomass).

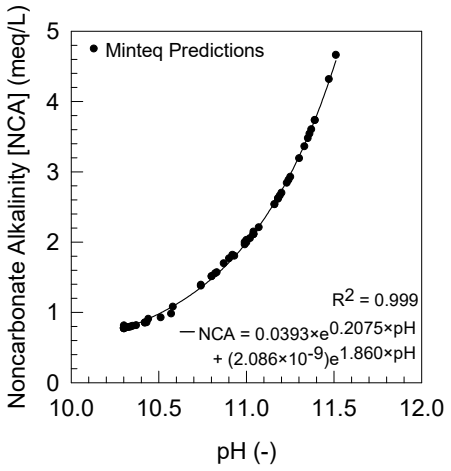

Figure 1. Predicted non-carbonate alkalinity in BG11 media as a function of pH based on Minteq.

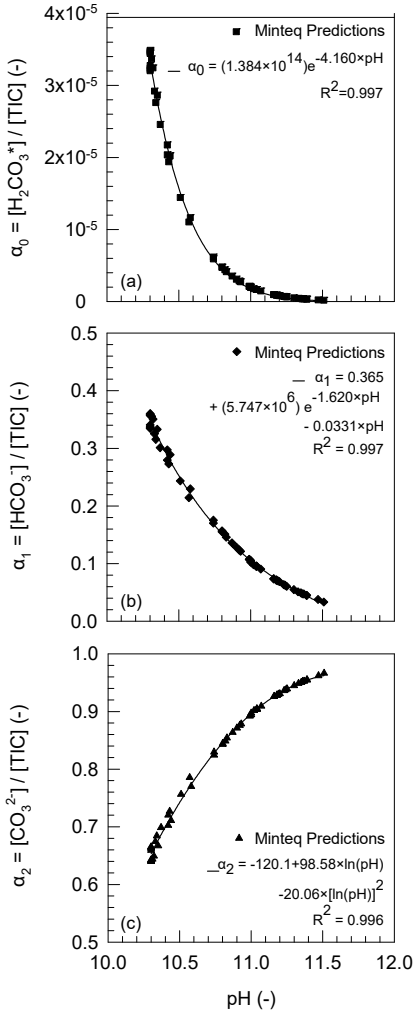

Figure 2. Predicted (A) H_2CO_3*, (B) HCO_3^-, and (C) CO_3^{2-} speciation as a function of pH.

RESULTS AND DISCUSSION

IMPACT OF IONIC STRENGTH AND NON-CARBONATE BUFFERS ON TIC CALCULATIONS

The ionic strength and presence of non-carbonate buffers impacted the TIC concentration calculated from Watson and Drapcho (2016) data (table 7). Over the range of added inorganic carbon studied (2.83 – 22.64 mg C/L), the calculated values of TIC based on total alkalinity measurements were 11.15 – 32.63 mg/L, representing 8.32 – 9.99 mg/L of excess TIC (table 6). After consideration of ionic strength, calculated TIC values were reduced 0.97 - 2.89 mg/L. Further, subtraction of non-carbonate alkalinity in the medium from total alkalinity before calculation of TIC led to an average reduction in initial TIC of 4.00 mg/L. The final calculated TIC values remained an average of 3.12 $\pm$ 0.25 mg/L TIC greater than the concentration of carbon added as Na_2CO_3.

Initial TIC in excess of added Na_2CO_3, at least in part, likely originated from atmospheric CO_2 upon reactor setup and was therefore bioavailable during experiments. Consistently, laboratory DI water, which was used to prepare BG11 media, was found to contain 1 mg/L of (bioavailable) TIC. In addition, media was exposed to atmospheric conditions during setup and initial adjustment of pH to 10.3. Using a dynamic model (Watson, 2009) with conditions representative of the 2016 experiments (e.g., atmospheric CO_2, reactor geometry, time for setup), it is estimated that up to 2 mg/L of bioavailable TIC could have diffused into reactors. Further, excess TIC (above added Na_2CO_3) was relatively constant (approximately 3 mg/L TIC), as would be expected for reactors at the same pH if the remaining TIC above added Na_2CO_3 originated from atmospheric diffusion.

RE-EVALUATION OF KINETIC PARAMETERS

Adjustment of TIC values to account for ionic strength and non-carbonate buffers had a substantial impact on Monod kinetic parameters. Revised estimates of μ_{max} values range from 0.051 to 0.060 hr^{-1} and are 17.6% to 28.2% less than reported in Watson and Drapcho (2016), depending on the TIC source (table 8). This range of maximum specific growth rate values aligns with Novak and Brune (1985), who reported a range of 0.046 to 0.057 hr^{-1} for *Scenedesmus* when assuming CO_2 to be the only TIC source.

Data adjustments also significantly impact K_S values (table 8). Half-saturation constants reflect the ease of use of the inorganic carbon species, with the least estimate of K_s obtained for CO_2 and the greatest for CO_3^{2-}. These K_S values are much less than Watson and Drapcho (2016) reported and generally lower than reported in the literature, likely due to differences in culture conditions of pH and light intensity (Novak and Brune, 1985; Chen and Durbin, 1994). However, the K_S for TIC was much greater than reported by Goldman et al. (1974) for pH 7.05 to 7.59, although they noted significant increases with only slight changes in pH. The K_S for TIC was on par with those reported by Caperon and Smith (1978) of 4.3 – 5.3 mg/L C.

Table 7. Analysis of initial TIC in each reactor, as compared to added Na_2CO_3 and that reported in Watson and Drapcho (2016).

TIC added as Na_2CO_3 (mg/L C)	Previously Reported (mg/L C)		Calculated in Current Work (mg/L C)		
	TIC from Watson and Drapcho (2016)[a]	Excess TIC	TIC corrected For ionic strength[b]	TIC corrected for non-carbonate buffers[c]	TIC above added Na_2CO_3[d]
2.83	11.15	8.32	10.18	6.16	3.33
5.66	14.19	8.53	13.00	8.73	3.07
8.49	17.23	8.74	15.87	11.86	3.37
11.32	20.32	9.00	18.69	14.70	3.37
14.15	22.77	8.62	20.76	16.82	2.67
16.98	26.28	9.30	23.94	20.02	3.04
19.81	29.21	9.40	26.61	22.70	2.89
22.64	32.63	9.99	29.74	25.84	3.20

[a] Values calculated using total alkalinity and pH measurements;
[b] Values after ionic strength corrections
[c] Values after subtraction of non-carbonate buffers;
[d] Unaccounted for TIC is expected to have been bioavailable, resulting from diffusion of atmospheric CO_2 prior to experimental time zero.

Table 8. Adjusted Monod kinetic parameters for TIC-limited freshwater algal growth, as compared to Watson and Drapcho (2016) data.

	Watson and Drapcho (2016)		Updated Trial 1 (0.05, 0.10, 0.15 g/L Na_2CO_3 reactors)			Updated Trial 2 (0.025, 0.075, 0.125, 0.175 g/L Na_2CO_3)			Updated Trial 1 and 2 Average	
Substrate	μ_{max} (hr^{-1})	K_S (mg/L C)	μ_{max} (hr^{-1})	K_S (mg/L C)	R^2	μ_{max} (hr^{-1})	K_S (mg/L C)	R^2	μ_{max} (hr^{-1})	K_S (mg/L C)
CO_2	0.073	5.36×10^{-4}	0.061	9.80×10^{-5}	0.96	0.058	2.35×10^{-4}	0.92	0.060	1.67×10^{-4}
HCO_3^-	0.073	6.84	0.057	1.03	0.95	0.057	2.61	0.92	0.057	1.81
CO_3^{2-}	0.071	10.44	0.052	1.81	0.94	0.050	4.42	0.92	0.051	3.12
TIC	0.073	17.52	0.053	2.77	0.94	0.052	6.97	0.92	0.053	4.88

RE-EVALUATING STOICHIOMETRIC PARAMETERS

While biomass elemental composition was unchanged from Watson and Drapcho (2016), relationships based on initial TIC were slightly altered. Biomass carbon and nitrogen contents still increased linearly with increasing initial TIC, although with greater slopes (table 9). Biomass phosphorous content still exhibited a quadratic relationship with initial TIC, increasing initially but then decreasing in the 0.15 and 0.20 g/L Na_2CO_3 reactors.

Molar representations of algal biomass (table 10) remained unchanged from Watson and Drapcho (2016) (table 10). Indeed, molar C:N ratios still ranged from 6.09 to 6.68, depending on the reactor, which aligned well with Redfield's marine (Redfield, 1934) and laboratory *Scenedesmus* data (table 3). Due to the high phosphate content in BG11, biomass across reactors had a high phosphorous content, likely due to polyphosphate accumulation, as was demonstrated by Geider and La Roche (2002). As such, molar C:P and N:P were much below Redfield's reports.

Estimates of cellular molecular mass were improved by considering deviations from the traditional elemental model for algal biomass (table 10). When calculated based on $(CH_2O)_x(NH_3)_y(H_3PO_4)_z$, the molecular mass of algal cells ranged from 300 to 428 mg/mmol in Watson and Drapcho (2016). However, the true molecular mass calculated based on the measured mass-percent of carbon in cells (eq. 13) ranged from 346 to 474 mg/mmol. As the true molecular masses are higher than anticipated by the traditional elemental model $[(CH_2O)_x(NH_3)_y(H_3PO_4)]$, it is expected that cells did contain notable quantities of micronutrients. It is possible that the excess cellular mass originated from hydrogen and oxygen; however, the traditional elemental model is more likely to overestimate, rather than under-estimate, cellular hydrogen and oxygen (Anderson, 1995).

Adjustments to TIC and cellular molecular mass calculations led to better alignment between theoretical and observed biomass yields (table 10). Theoretical and observed biomass yields were 4.52 $\pm$ 0.57 and 4.42 $\pm$ 0.58 mg/mg, 17% and 30% less than Watson and Drapcho (2016) reported, respectively. Notably, the adjusted observed biomass yield is only 2% greater than the theoretical biomass yield. Despite the reduction in estimates, biomass yields are higher than reported by Goldman et al. (1974) for *Scendesmus* and calculated from Ketchum and Redfield (1949) data (table 3) (2.06 – 2.26 mg biomass/mg C), likely due to differences in growth phases, cellular phosphorous accumulation, and provided TIC (as described in detail by Watson and Drapcho, 2016).

PRACTICAL IMPLICATIONS

The current work outlines a computational, low-cost method for calculating TIC from total alkalinity measured in complex BG11 media. While other methodologies are available for direct measurement of CO_2 (e.g., via carbon analyzer) and carbonates (i.e., ion chromatography), their use may be cost- prohibitive and may not provide greater accuracy at the inorganic carbon concentrations found in algal cultures. As BG11 is a common growth medium, the empirical relationships between pH, non-carbonate alkalinity (fig. 1), and ionization fractions (fig. 2) can be used with reasonable confidence by other researchers. Inherent in the use of figures 1-2 is that samples are filtered with 0.2 µm filters before titration, and low biomass production occurs, such that algal growth does not change ammonia and phosphate alkalinities appreciably. However, measurement of ammonia and phosphate during growth would allow for quick adjustment of the non-carbonate alkalinity from figure 1.

Table 9. Relationship between adjusted initial TIC (mg/L C) and biomass elemental composition on a mass-basis, applicable over range 2.83 -22.6 mg/L TIC, as compared to Watson and Drapcho (2016).

Macronutrient	Watson and Drapcho (2016)	R^2	Updated Based on Adjusted Data	R^2
Carbon	%C = 0.366 × (Initial TIC) + 14.1	0.999	%C = 0.388 × (Initial TIC) + 15.8	0.999
Nitrogen	%N = 0.505 × (Initial TIC) +2.94	0.918	%N = 0.0532 × (Initial TIC) + 3.18	0.908
Phosphorous	%P = -0.0153 × (Initial TIC)^2 + 0.163 × (Initial TIC) + 2.55	0.935	%P = -0.0169 × (Initial TIC)^2 + 0.486 × (Initial TIC) + 5.16	0.930

Table 10. Adjusted stoichiometric parameters describing TIC-limited freshwater algal growth, as compared to Watson and Drapcho (2016).

	Molar Ratios			Based on Adjusted Data			Watson and Drapcho (2016)		
Added Na_2CO_3 (g/L)	C:N	C:P ("x")	N:P ("y")	Molecular Mass (g/mol)	$Y_{theoretical}$ (mg/mg)	$Y_{observed}$ (mg/mg)	Molecular Mass (g/mol)	$Y_{theoretical}$ (mg/mg)	$Y_{observed}$ (mg/mg)
0.05	6.09	6.16	1.01	386.2	5.22	4.92	300.0	4.06	5.13
0.10	6.34	6.18	0.974	345.7	4.66	3.95	299.3	4.04	6.39
0.15	6.14	7.67	1.25	396.6	4.31	4.92	353.5	3.84	6.76
0.20	6.68	10.16	1.52	473.6	3.88	3.58	428.3	3.52	5.95

Based on a synthesis of the literature on CCMs, variable C:N:P, and the nutrient-H^+ compensation principle, general stoichiometric algal growth equations are presented. Researchers can easily convert their measured C:N:P into a balanced stoichiometric equation to predict the impact of algal growth on culture pH and alkalinity. Stoichiometric relationships between macronutrient uptake and culture conditions were congruent with the nutrient-H^+ principle presented by Wolf-Gladrow (2007). Work from Anderson (1995), Grobbelaar (2004), and Prochazkova et al. (2014) were integrated to describe when consideration of cellular elements other than C:N:P is needed. Importantly, a method for estimating the molecular mass of biomass without knowledge of non-C:N:P elements is presented (eq. 13), such that biomass production on a mass-basis can be estimated based only on inorganic carbon uptake.

Through improved TIC and cellular molecular mass calculations from Watson and Drapcho (2016) data, accurate estimates of kinetic and stoichiometric parameters for mixed *Scenedesmus* cultures are presented. Estimates of μ_{max} and K_S values were reduced from those previously presented, with μ_{max} for CO_2 very close to value reported by Novak and Brune (1985). Estimates of $Y_{theoretical}$ and $Y_{observed}$ were much closer aligned after TIC data adjustment. Many literature sources report algal growth parameters based on a single inorganic carbon source. This is the first report that provides growth parameters based on multiple inorganic carbon sources at high pH.

All contributions support the basis for the development of a dynamic algal growth model that can be used to design high-pH systems to support carbon abatement and biomass production. Existing models often assume TIC to be non-limiting (e.g., Davidson and Gurney, 1999), only consider CO_2 or HCO_3^- as a single substrate (e.g., Liehr et al., 1988; Eze et al., 2018), or assume equilibrium conditions (e.g., James and Boriah, 2010). However, systems for carbon abatement would be intentionally designed for inorganic-carbon-limited conditions, and high pH operation would necessitate that the role of CO_3^{2-} for algal growth (if any) be elucidated. Also, CCMs are expected to disturb carbonate equilibria (e.g., Ludden et al., 1985), so conversion rates between species must be considered. As such, adjusted growth parameters and stoichiometric reactions can be used to formulate differential mass balances that capture the complex chemical and biological rates impacting biomass production, inorganic carbon utilization, pH, and alkalinity, as was originally proposed by Watson and Drapcho (2016).

Conclusion

The contributions presented provide the foundation for a dynamic mathematical model to support the design of high pH algal carbon capture systems. First, a computational method was developed to more accurately calculate TIC in BG11 media based on total alkalinity and pH by accounting for the presence of non-carbonate buffers. Non-carbonate alkalinity in BG11 media increased exponentially with increasing pH, based on Minteq analysis, with empirical relationships presented (figs. 1-2) to support translation by other researchers. Improved TIC calculations allowed for a more accurate estimate of kinetic parameters (μ_{max} and K_S values) describing TIC-limited freshwater algal growth. This is the only known report considering the kinetics of multiple inorganic carbon sources.

Second, literature was synthesized to present stoichiometric algal growth equations that account for multiple inorganic carbon sources and variable nutrient ratios. This analysis shows that although nitrate uptake is known to increase alkalinity (1 mol equivalent/mol N), phosphate uptake, regardless of species, also increases alkalinity (1 mol equivalent/mol P).

Further, although the traditional model of algal biomass $[(CH_2O)_x(NH_3)_y(H_3PO_4)_z]$ is known to overestimate hydrogen and oxygen and neglect micronutrient content, it can be used confidently to estimate macronutrient uptake and subsequent shifts in pH and alkalinity. When calculating mass-based biomass yield, the traditional model of algal biomass should not be used. Rather, a molecular mass based on direct measurement of carbon content led to a close alignment of observed and theoretical biomass yields, based on Watson and Drapcho (2016) data.

Acknowledgments

This material is based upon work supported by the National Science Foundation under Grant No. 2219258: MCA - Exploring Algal Carbon Capture Potential in High pH Laboratory- and Field-Scale Systems. Any opinions, findings, and conclusions or recommendations expressed in this material are those of the authors and do not necessarily reflect the views of the National Science Foundation. Financial support for Elizabeth Flanagan was provided by an assistantship provided by the EEES Department at Clemson University.

References

Anderson, L. A. (1995). On the hydrogen and oxygen content of marine phytoplankton. *Deep Sea Res. Part I, 42*(9), 1675-1680. https://doi.org/10.1016/0967-0637(95)00072-E

APHA. (1995). Standard methods for the examination of water and wastewater. *19th*. American Public Health Association.

Ataeian, M., Liu, Y., Canon-Rubio, K. A., Nightingale, M., Strous, M., & Vadlamani, A. (2019). Direct capture and conversion of CO2 from air by growing a cyanobacterial consortium at pH up to 11.2. *Biotechnol. Bioeng., 116*(7), 1604-1611. https://doi.org/10.1002/bit.26974

Auguères, A.-S., & Loreau, M. (2015). Regulation of Redfield ratios in the deep ocean. *Global Biogeochem. Cycles, 29*(2), 254-266. https://doi.org/10.1002/2014GB005066

Bhatti, S., & Colman, B. (2008). Inorganic carbon acquisition in some synurophyte algae. *Physiol. Plant., 133*(1), 33-40. https://doi.org/10.1111/j.1399-3054.2008.01061.x

Boyd, C. E., Tucker, C. S., & Somridhivej, B. (2016). Alkalinity and hardness: Critical but elusive concepts in aquaculture. *J. World Aquacult. Soc., 47*(1), 6-41. https://doi.org/10.1111/jwas.12241

Brewer, P. G., & Goldman, J. C. (1976). Alkalinity changes generated by phytoplankton growth. *Limnol. Oceanogr., 21*(1), 108-117. https://doi.org/10.4319/lo.1976.21.1.0108

Burlew, J. S. (1953). Algal culture from laboratory to pilot plant. Carnegie Inst. Washington Publ.

Caperon, J., & Smith, D. F. (1978). Photosynthetic rates of marine algae as a function of inorganic carbon concentration. Limnology and Oceanography, 23(4), 704-708.
Chen, C. Y., & Durbin, E. G. (1994). Effects of pH on the growth and carbon uptake of marine phytoplankton. *Mar. Ecol. Prog. Ser., 109*(1), 83-94. https://doi.org/10.3354/meps109083
Colman, B., Huertas, I. E., Bhatti, S., & Dason, J. S. (2002). The diversity of inorganic carbon acquisition mechanisms in eukaryotic microalgae. *Funct. Plant Biol., 29*(3), 261-270. https://doi.org/10.1071/PP01184
Cooper, T. G., Filmer, D., Wishnick, M., & Lane, M. D. (1969). The active species of "CO2" utilized by ribulose diphosphate carboxylase. *J. Biol. Chem., 244*(4), 1081-1083. https://doi.org/10.1016/S0021-9258(18)91899-5
Danckwerts, P. V. (1970). *Gas-liquid reactions.* New York: McGraw-Hill Book Co.
Davidson, K., & Gurney, W. S. (1999). An investigation of non-steady-state algal growth. II. Mathematical modelling of co-nutrient-limited algal growth. *J. Plankton Res., 21*(5), 839-858. https://doi.org/10.1093/plankt/21.5.839
Dickson, A. G. (1981). An exact definition of total alkalinity and a procedure for the estimation of alkalinity and total inorganic carbon from titration data. *Deep Sea Res. Part I Oceanogr. Res. Pap., 28*(6), 609-623. https://doi.org/10.1016/0198-0149(81)90121-7
Dickson, A. G. (1992). The development of the alkalinity concept in marine chemistry. *Mar. Chem., 40*(1), 49-63. https://doi.org/10.1016/0304-4203(92)90047-E
Drapcho, C. M., & Brune, D. E. (2000). The partitioned aquaculture system: Impact of design and environmental parameters on algal productivity and photosynthetic oxygen production. *Aquacult. Eng., 21*(3), 151-168. https://doi.org/10.1016/S0144-8609(99)00028-X
Eze, V. C., Velasquez-Orta, S. B., Hernández-García, A., Monje-Ramírez, I., & Orta-Ledesma, M. T. (2018). Kinetic modelling of microalgae cultivation for wastewater treatment and carbon dioxide sequestration. *Algal Research, 32*, 131-141. https://doi.org/10.1016/j.algal.2018.03.015
Felfoldy, L. (1960). Comparative studies on photosynthesis in different *Scenedesmus* strains. *Acta Botanica Hungarica, 6*, 1-13.
Geider, R., & La Roche, J. (2002). Redfield revisited: Variability of C:N:P in marine microalgae and its biochemical basis. *Eur. J. Phycol., 37*(1), 1-17. https://doi.org/10.1017/S0967026201003456
Goldman, J. C., & Brewer, P. G. (1980). Effect of nitrogen source and growth rate on phytoplankton-mediated changes in alkalinity 1. Limnology and Oceanography, 25(2), 352-357.
Goldman, J. C., Oswald, W. J., & Jenkins, D. (1974). The kinetics of inorganic carbon limited algal growth. *J. Water Pollut. Control Fed., 46*(3), 554-574. Retrieved from http://www.jstor.org/stable/25038157
Grobbelaar, J. U. (2004). Algal nutrition: Mineral nutrition. In A. Richmond (Ed.), *Handbook of microalgal culture: Biotechnology and applied phycology* (pp. 97-115).
Gustafsson, J. P. (2011). Visual MINTEQ 3.0 user guide. Stockholm, Sweden: KTH, Department of Land and Water Recources.
Hillebrand, H., Steinert, G., Boersma, M., Malzahn, A., Meunier, C. L., Plum, C., & Ptacnik, R. (2013). Goldman revisited: Faster-growing phytoplankton has lower N:P and lower stoichiometric flexibility. *Limnol. Oceanogr., 58*(6), 2076-2088. https://doi.org/10.4319/lo.2013.58.6.2076
James, S. C., & Boriah, V. (2010). Modeling algae growth in an open-channel raceway. *J. Comput. Biol., 17*(7), 895-906. https://doi.org/10.1089/cmb.2009.0078
Ketchum, B. H., & Redfield, A. C. (1949). Some physical and chemical characteristics of algae growth in mass culture. *J. Cell. Comp. Physiol., 33*(3), 281-299. https://doi.org/10.1002/jcp.1030330303
King, D. L. (1970). The role of carbon in eutrophication. *J. Water Pollut. Control Fed., 42*(12), 2035-2051. Retrieved from http://www.jstor.org/stable/25036835
Liehr, S. K., Eheart, J. W., & Suidan, M. T. (1988). A modeling study of the effect of pH on carbon limited algal biofilms. *Water Res., 22*(8), 1033-1041. https://doi.org/10.1016/0043-1354(88)90151-0
Lindsey, R. (2021). Climate change: Atmospheric carbon dioxide. Retrieved from https://www.climate.gov/news-features/understanding-climate/climate-change-atmospheric-carbon-dioxide
Ludden, E., Admiraal, W., & Colijn, F. (1985). Cycling of carbon and oxygen in layers of marine microphytes; a simulation model and its eco-physiological implications. *Oecologia, 66*(1), 50-59. https://doi.org/10.1007/BF00378551
NOAA. (2021). Despite pandemic shutdowns, carbon dioxide and methane surged in 2020. Retrieved from https://research.noaa.gov/article/ArtMID/587/ArticleID/2742/Despite-pandemic-shutdowns-carbon-dioxide-and-methane-surged-in-2020
Novak, J. T., & Brune, D. E. (1985). Inorganic carbon limited growth kinetics of some freshwater algae. *Water Res., 19*(2), 215-225. https://doi.org/10.1016/0043-1354(85)90203-9
Office of Fossil Energy & Carbon Management. (2022). Office of Carbon Management. Retrieved from https://www.energy.gov/fecm/office-carbon-management
Osterhout, W. J., & Haas, A. R. (1918). On the dynamics of photosynthesis. *J. Gen. Physiol., 1*(1), 1-16. https://doi.org/10.1085/jgp.1.1.1
ÖSterlind, S. (1948). The retarding effect of high concentrations of carhon dioxide and carhonate ions on the growth of a green alga. *Physiol. Plant., 1*(2), 170-175. https://doi.org/10.1111/j.1399-3054.1948.tb07121.x
Paulmier, A., Kriest, I., & Oschlies, A. (2009). Stoichiometries of remineralisation and denitrification in global biogeochemical ocean models. *Biogeosciences, 6*(5), 923-935. https://doi.org/10.5194/bg-6-923-2009
Planavsky, N. J. (2014). The elements of marine life. *Nat. Geosci., 7*(12), 855-856. https://doi.org/10.1038/ngeo2307
Portielje, R., & LiJklema, L. (1995). Carbon dioxide fluxes across the air-water interface and its impact on carbon availability in aquatic systems. *Limnol. Oceanogr., 40*(4), 690-699. https://doi.org/10.4319/lo.1995.40.4.0690
Procházková, G., Brányiková, I., Zachleder, V., & Brányik, T. (2014). Effect of nutrient supply status on biomass composition of eukaryotic green microalgae. *J. Appl. Phycol., 26*(3), 1359-1377. https://doi.org/10.1007/s10811-013-0154-9
Redfield, A. C. (1934). On the proportions of organic derivatives in sea water and their relation to the composition of plankton. 176-192. Liverpool: University Press of Liverpool.
Reichle, D., Houghton, J., Kane, B., Ekmann, J., Benson, S., Clarke, J., et al., Carbon
Sequestration Research and Development, available at: osti.gov/servlets/purl/810722
Richards, F. A. (1965). Anoxic basins and fjords. In J. P. Riley, & G. Skirrow (Eds.), *Chemical oceanography* (pp. 611-643). New York: Academic Press.
Singh, U. B., & Ahluwalia, A. S. (2013). Microalgae: A promising tool for carbon sequestration. *Mitig. Adapt. Strateg. Glob. Change, 18*(1), 73-95. https://doi.org/10.1007/s11027-012-9393-3
Smith, S. V. (1985). Physical, chemical and biological characteristics of CO2 gas flux across the air-water interface.

Plant Cell Environ., 8(6), 387-398. https://doi.org/10.1111/j.1365-3040.1985.tb01674.x

Stumm, Werner, and James J. Morgan. (1996). Aquatic chemistry: chemical equilibria and rates in natural waters. John Wiley & Sons, 2012.

Stumm, W., & Morgan, J. J. (1996). Aquatic chemistry: Chemical equilibria and rates in natural waters. (3rd edition) John Wiley & Sons.

Touloupakis, E., Cicchi, B., Benavides, A. M., & Torzillo, G. (2016). Effect of high pH on growth of *Synechocystis* sp. PCC 6803 cultures and their contamination by golden algae (*Poterioochromonas* sp.). *Appl. Microbiol. Biotechnol., 100*(3), 1333-1341. https://doi.org/10.1007/s00253-015-7024-0

Vadlamani, A., Viamajala, S., Pendyala, B., & Varanasi, S. (2017). Cultivation of microalgae at extreme alkaline pH conditions: A novel approach for biofuel production. *ACS Sustain. Chem. Eng., 5*(8), 7284-7294. https://doi.org/10.1021/acssuschemeng.7b01534

Wang, J., & Curtis, W. R. (2016). Proton stoichiometric imbalance during algae photosynthetic growth on various nitrogen sources: Toward metabolic pH control. *J. Appl. Phycol., 28*(1), 43-52. https://doi.org/10.1007/s10811-015-0551-3

Watson, M. K., & Drapcho, C. M. (2016). Kinetics of inorganic carbon-limited freshwater algal growth at high pH. *Trans. ASABE, 59*(6), 1633-1643. https://doi.org/10.13031/trans.59.11520

Watson, M. K. (2009). Growth and modeling of freshwater algae as a function of media inorganic carbon content (Masters thesis, Clemson University).

Wolf-Gladrow, D. A., Zeebe, R. E., Klaas, C., Körtzinger, A., & Dickson, A. G. (2007). Total alkalinity: The explicit conservative expression and its application to biogeochemical processes. *Mar. Chem., 106*(1), 287-300. https://doi.org/10.1016/j.marchem.2007.01.006